Journal of Radiation Research and Applied Sciences 18 (2025) 102052

Contents lists available at ScienceDirect

Journal of Radiation Research and Applied Sciences

journal homepage: www.journals.elsevier.com/journal-of-radiation-research-and-applied-sciences

Honokiol modulates invasion and autophagy in pancreatic cancer via the miR-101/QKI axis in cancer-associated fibroblasts

Liang Chu [a], Bin Yu [a], Zhe Jiang [a], Zan Liu [b], Yunmei Wang [c,*], Yuqin Hu [d,**]

[a] Department of ITC&WM Oncology, Shaanxi Provincial Cancer Hospital Affiliated to Medical School, Xi'an Jiao Tong University, Xi'an, Shaanxi, 710061, China
[b] Department of Oncology, Xi'an Gaoxin Hospital, Xi'an, Shaanxi, 710061, China
[c] Department of Medical Oncology, Shaanxi Provincial Cancer Hospital Affiliated to Medical School, Xi'an Jiao Tong University, Xi'an, Shaanxi, 710061, China
[d] Outpatient and Emergency Department of Medical Oncology, Shaanxi Provincial Cancer Hospital Affiliated to Medical School, Xi'an Jiao Tong University, Xi'an, Shaanxi, 710061, China

ARTICLE INFO

Keywords:
Honokiol
Pancreatic cancer
Cancer-associated fibroblasts
Autophagy
miR-101
Tumor microenvironment
PDAC therapy

ABSTRACT

Background: Cancer-associated fibroblasts (CAFs) promote the pathological process of pancreatic ductal adenocarcinoma (PDAC), a highly aggressive malignant tumor. Autophagy plays a dual role in cancer, and in the context of PDAC, increased autophagy significantly promotes PDAC cell survival and metastasis. We aimed to investigate whether honokiol, a naturally occurring compound with anti-cancer properties, regulated the *miR-101*/QKI axis to suppress CAF-mediated autophagy, proliferation, and invasion in PDAC.

Methods: CAFs isolated from PDAC specimens were treated with honokiol to evaluate its effects on the tumor microenvironment. Conditioned medium from honokiol-treated CAF was used to incubate with PDAC cells, and their malignant phenotypes (proliferation, invasion, autophagy) were assessed through a series of *in vitro* and *in vivo* functional assays. Molecular analyses elucidated honokiol/miR-101/QKI axis driving PDAC pathogenesis. Honokiol therapeutic validation conducted using a mouse xenograft model.

Results: MiR-101 expression was significantly downregulated in CAFs (~2.8-fold), whereas QKI and α-SMA were upregulated (~2.8-fold and ~3.2-fold, respectively). Honokiol treatment (50 μM) enhanced *miR-101* expression (~2.5-fold), reduced QKI and α-SMA level (~60 % and ~55 % reduction, respectively) in CAFs. Conditioned media from honokiol-treated CAFs substantially suppressed PDAC cell autophagy, proliferation, migration, and invasion. Mechanistically, honokiol attenuated malignant PDAC cell phenotypes by inducing miR-101 expression in CAFs. QKI was identified as a miR-101 target in CAFs. MiR-101 overexpression in CAFs inhibited PDAC cell malignant behavior through QKI silencing. In mouse xenograft models, honokiol suppressed tumorigenesis by modulating *miR-101*/QKI axis.

Conclusion: Honokiol inhibits CAF-induced autophagy, proliferation, migration, and invasion in PDAC by regulating the miR-101/QKI axis, thereby modifying cancer cell behavior. This reveals the potential of honokiol as a promising therapeutic agent to remodel the tumor microenvironment and suppress pancreatic cancer progression.

1. Introduction

Pancreatic carcinoma (PC) is a highly metastatic malignant tumor of the digestive tract. Pancreatic ductal adenocarcinoma (PDAC) is the most common type of PC, accounting for more than 90 % of cases. Its most prominent features are dense fibrous interstitial reaction and metabolic dysfunction in the tissue microenvironment (Miller et al., 2018). Due to its often-unnoticed onset and the lack of effective biomarkers to screen for it, most patients are diagnosed only after PC has metastasized. In addition, few patients benefit from surgical resection and the 5-year survival rate of PC patients is only 6 % (Gillen et al., 2010). Combinations of chemotherapy drugs (e.g., gemcitabine) are still the main treatment for most metastatic PC patients (DeSantis et al., 2014). However, the use of first-line chemotherapy drugs, including

* Corresponding author. No. 309, Yanta West Road, Yanta District, Xi'an, Shaanxi, 710061, China.
** Corresponding author. No. 309, Yanta West Road, Yanta District, Xi'an, Shaanxi, 710061, China.
E-mail addresses: shuic_1999@163.com (L. Chu), yuyu2627558@163.com (B. Yu), paradise1912@sina.com (Z. Jiang), www.lzbb1981@126.com (Z. Liu), Onco_yunmei@163.com (Y. Wang), 13379255770@163.com (Y. Hu).

https://doi.org/10.1016/j.jrras.2025.102052
Received 25 August 2025; Received in revised form 23 October 2025; Accepted 27 October 2025
Available online 10 November 2025

gemcitabine, is often more likely to produce drug resistance than long-lasting remission, and the resulting possibility of tumor recurrence and metastasis is very high; PDAC is highly aggressive and can spread to lymph nodes, liver, abdominal cavity, lung or intestine, and these factors severely limit the effectiveness of gemcitabine (Beutel & Halbrook, 2023; Kim et al., 2023). Numerous studies in the fields of genetics and epigenetics have identified key genetic changes leading to the occurrence of PDAC, including mutations in *KRAS*, *P53*, *BRCA1*, *BRCA2*, and *SMAD4* (Thomas & Radhakrishnan, 2019). However, targeting these genetic or epigenetic signatures has not yet produced improved treatments for PDAC, underscoring the urgent need for alternative therapeutic strategies. This therapeutic impasse has shifted focus towards the tumor microenvironment (TME), a key contributor to PDAC's aggressive nature and treatment resistance (Niu et al., 2024). The dense stromal compartment, constituting up to 90 % of the tumor volume, acts as a physical and functional barrier that impedes drug delivery, promotes tumorigenesis, and fosters an immunosuppressive niche (Hosein et al., 2020). Therefore, targeting stromal components, particularly cancer-associated fibroblasts (CAFs), has emerged as a promising avenue to disrupt this pro-tumorigenic crosstalk and improve therapeutic outcomes.

Intratumoral metabolic communication mechanisms can symbiotically support tumor metabolism, maintenance and growth, or competitively weaken anti-tumor immunity (Chapman & Chi, 2024). The TME is critically important to the occurrence, development and prognosis of PDAC (Melstrom et al., 2017). In the TME, CAFs, an important component of the pancreatic stromal cell population, have attracted extensive attention in the field of PDAC treatment because of their interaction with PDAC cells and their participation in the process of PC fibrosis (Niu et al., 2024; Rebelo et al., 2023). The interaction between CAFs and PDAC cells can not only promote tumor progression and metastasis, but also maintain their own activation, thus forming a positive feedback loop to aggravate tumorigenesis and drug resistance (Wang, Yang, et al., 2020). Increased PDAC cell death was observed when cancer cells were isolated from the extracellular matrix *in vitro*, indicating that the cells depend on their environment. However, when cancer cells were cultured with laminin or fibronectin, the survival rate of PDAC was significantly improved (Shi et al., 2019). In addition, the metabolic regulation and reprogramming of TMEs also affect the pathological processes of PC, among which autophagy plays an important role in the metabolic regulation the cancer cells (Biffi & Tuveson, 2021). In the metabolically active and nutrient-scarce TME, autophagy is a critical survival mechanism. In stromal cells, particularly CAFs, elevated autophagy facilitates the degradation of intracellular components to generate recycled nutrients (e.g., amino acids, fatty acids) and energy precursors, which can be secreted and utilized by neighboring cancer cells to support their growth and survival—a process known as metabolic coupling. Furthermore, autophagy in CAFs regulates the secretion of protumorigenic cytokines, growth factors, and extracellular matrix components, thereby fostering a metastatic niche and conferring resistance to chemotherapy. Consequently, both tumor cells and stromal cells can promote tumor progression and treatment resistance through autophagy-dependent secretion and metabolic reprogramming (New & Thomas, 2019). Therefore, exploring the mechanism of CAFs regulating autophagy to affect the TME of PDACs may elucidate a critical mechanism of how TME affects the progression of PC.

MicroRNAs (miRNAs) are non-coding RNAs which are typically 21–25 bases in length and can play a negative regulatory role through the complementary binding of the 3′-untranslated region (3′-UTR) of the target mRNA, inducing degradation or translational inhibition of the target mRNA to downregulate its expression (Carthew & Sontheimer, 2009). Aberrant miRNA expression is usually accompanied by a dysregulation of cellular regulation, including uncontrolled cell proliferation, failure of tumor suppressors, angiogenesis and metastasis (Dragomir et al., 2022). The effects of miRNAs on the TME have been investigated and studies have found that miRNAs can induce normal fibroblasts (NFs) to convert into CAFs by targeting various signaling pathways and metabolic substrates (Fang et al., 2025). Some miRNAs are also involved in the complex network signaling between tumor cells and CAFs, thus participating in tumorigenesis, metastasis and drug resistance (Peng et al., 2017). Knockdown of *miR-1* in NFs causes them to transform into CAF-like fibroblasts, which acts through the FOXO3a/VEGF/CCL2 signaling pathway (Shen et al., 2016). In NFs, *miR-21* can bind to the 3′-UTR of *SMAD7* mRNA and inhibit its translation, thereby increasing the phosphorylation level of SMAD2/3 and activating NFs through the SMAD2/3 and TGF-β1 signaling pathways (Li et al., 2013). In head and neck tumors, overexpression of *miR-7* in NFs can downregulate the target gene *RASSF2* and induce the activation of NFs into CAFs (Shen et al., 2017). Previous studies have noted the low expression of *miR-101* in CAFs and related tumor cells, where it has been shown to impair pro-tumorigenic functions. For instance, in lung cancer, *miR*-101 in CAFs inhibits tumor cell crosstalk by targeting CXCL12, and in hepatocellular carcinoma, it targets TGFBR1 to suppress vascular mimicry (Eun et al., 2023; Zhang, Liu, et al., 2015). Given its established role in regulating autophagy and its documented downregulation in PDAC, we hypothesized that *miR*-101 could be a critical mediator of CAF function in the pancreatic TME. In addition, the expression of *miR-101* is low in PC and its upregulation can accelerate the apoptosis and death of PDAC cells. Therefore, in-depth study of the function of *miR-101* in CAFs and its potential regulatory pathways is necessary to improve the prognosis and develop novel potential therapeutic strategies for PDAC.

Honokiol is a natural phenolic compound extracted from the leaves and bark of *Magnolia officinalis* and has a variety of pharmacological activities, including anti-inflammatory, anti-virus, anti-tumor and anti-angiogenesis (Arora et al., 2012). Honokiol can inhibit the expression of *EZH2* at both the mRNA and protein level through transcriptional regulation, providing a new strategy for the treatment of bladder cancer (Zhang, Zhao, et al., 2015). Honokiol inhibits epithelial-mesenchymal transition of breast cancer cells by targeting STAT3/Zeb1/E-cadherin axis (Avtanski et al., 2014). Honokiol inhibits spheroid formation of side population cells and xenograft growth of oral cancer and inhibits JAK/STAT signaling pathway and induces apoptosis (Huang et al., 2016). Surprisingly, honokiol can regulate the expression level of miR-101 and interfere with the pathological process of PDAC (Wang, Liu, et al., 2020). However, whether honokiol regulates the PDAC microenvironment through *miR-101* is still unclear.

In this study, we aimed to determine whether honokiol remodels CAF-mediated tumorigenesis by regulating PDAC cell proliferation, invasion and autophagy via the miR-101-QKI signaling axis. Our data establishes the scientific basis for the potential relevance of new therapeutic targets to treat PDAC and further drug development of a natural compound.

2. Materials and methods

2.1. Extraction and isolation of primary pancreatic CAFs

Tissue blocks used for primary CAF extraction were obtained from freshly resected pancreatic cancer samples from patients diagnosed with PDAC (No neoadjuvant chemotherapy or radiotherapy prior to surgery) in clinical. Specimens were placed in 15 mL centrifuge tubes of whole culture in DMEM/F12 containing high concentration of phosphate-buffered saline (PBS) as soon as possible after collection, stored at 4 °C or on ice and processed within 24 h. The tissue blocks were placed on a plate and rinsed thoroughly twice with PBS, followed by two thorough washes. The cleaned tissue block was placed in PBS and sterilized surgical scissors were used to remove fat and vascular tissue while retaining as much as possible of the solid tumor tissue. The solid tumor tissue was cut into small pieces of ~500 mm^2 and placed in 6-well plates, and approximately half of the tissue was added to DMEM/F12 for whole culture at 37 °C in 5 % CO_2. The fresh whole culture medium was replaced every day. When the long fusiform CAF extruded out of the

tissue block, 0.05 % Trypsin was added. The solution containing the exfoliated CAFs was transferred to a new 15 mL centrifuge tube and centrifuged at 1000 RPM to isolate cells from debris.

2.2. Cell culture and treatment

PDAC cell lines PANC-1 and Paca-2 as well as primary CAFs and NFs were cultured in DMEM containing 15 % FBS and 1 % penicillium-streptomycin at 37 °C in a humidified atmosphere containing 5 % CO_2. Approximately 2×10^6 stably transfected CAFs were cultured in 10 cm cell culture dishes for 48 h. CAFs were treated with different doses of honokiol (0, 12.5, 25, 50 or 100 μM) for 72 h (Wang, Liu, et al., 2020). Honokiol-treated cells were harvested and cultured in complete DMEM medium (5×10^5 cells) for 12 h. Finally, the cells were centrifuged and the medium was collected. Cells were cultured in conditioned medium (CM) for 2 weeks before subsequent cytological experiments.

2.3. qRT-PCR

Total RNA was extracted from cells using TRIzol reagent (Takara). This RNA served as a template for reverse transcription, which was carried out with the Prime Script RT reagent Kit to synthesize cDNA. The RT-qPCR was performed using parameters optimized for an ABI 7900HT RT-PCR system with the SYBR Premix Ex *Taq*II kit. The expression levels of the target genes were quantified and normalized using the $2^{-\Delta\Delta CT}$ method.

2.4. Western blot assay

Cells were harvested, lysed with RIPA buffer and centrifuged to obtain the supernatant for protein quantification using the BAC method. SDS-PAGE was used to separate proteins, which were then transferred onto PVDF membranes. After blocking with 5 % nonfat milk for 2 h, membranes were incubated with diluted primary antibodies against α-SAM (1:1000, ab109197, abcam), FAP (1:1000, ab314456, abcam), FSP1 (1:1000, ab197896, abcam), GAPDH (1:1000, ab8245, abcam), QKI (1:1000, sc-517305, Santa-Cruz) or LC3I/II (1:1000, 4108, Cell Signaling Technology). After washing, membranes were incubated with secondary antibodies for 1 h at room temperature. Protein bands were visualized using a luminescent solution, then images were captured and analyzed with Image J software.

2.5. CCK-8

Cells were seeded into 96-well plates (3000 cells/well). Following incubation for 24, 48 or 72 h, the wells were refreshed by removing the existing supernatant and adding 100 μL of a mixture composed of DMEM/Nutrient Mixture F12 supplemented with 10 μL of the CCK-8. The cells were then incubated for an additional 2.5 h at 37 °C. After incubation, the plates were gently agitated for 10 min to ensure uniform distribution of the reagent and the OD was measured at a wavelength of 450 nm to assess cell proliferation.

2.6. Transwell assay

A 7:1 dilution of serum-free medium and Matrigel was applied to the upper chambers of a Transwell for invasion assays; migration assays were compared to chambers without Matrigel. PDAC cells (5×10^5 cells/mL) in 200 μL serum-free medium were seeded in the upper chamber, while 600 μL of complete medium was added to the lower chamber. After a 24 h incubation, non-invading cells on the Matrigel were removed and the chambers were fixed in 4 % paraformaldehyde (PFA) for 20 min and washed again, then the chambers were stained with crystal violet for 20 min, rinsed three times with PBS and air-dried. The number of cells that invaded or migrated was counted in five random fields under a microscope by ImageJ.

2.7. mRFP-GFP-LC3B indicator system

Briefly, PDAC cells were seeded in 6-well plates (2×10^5 cells/well). After 24 h, a double fluorescent mRFP-GFP-LC3B virus (MOI = 10; HanBio, Shanghai) was diluted with serum-free cell culture medium and 1 mL of virus dilution was added to each well. After incubation for 2 h, the medium was changed to complete medium. After 24 h, cells were passaged and seeded in small confocal dishes. After continuous culture for 24 h, the medium in the small dish was aspirated, cells were washed twice with PBS, cells were fixed with 4 % formaldehyde solution and the fluorescence was observed by confocal microscopy. Subsequently, autophagic flux was determined by evaluating the numbers of yellow fluorescent puncta (representing autophagosomes; GFP + RFP) and red fluorescent protein (RFP only; representing autolysosomes where the acid-sensitive GFP signal is quenched) puncta in at least 50 cells per condition from five random fields. The autophagic flux was calculated as the ratio of red-only puncta to total (yellow + red) LC3 puncta.

2.8. Transmission electron microscopy

For TEM analysis of autophagic structures, PDAC cells were treated with the respective CAF-CM for 48 h prior to fixation. Samples were fixed using a 2.5 % glutaraldehyde solution, rinsed with PBS twice and then stained with 1 % osmium tetroxide. After staining, cells underwent a series of ethanol washes for dehydration and were embedded in epoxy resin. The samples were placed in capsules and subjected to polymerization at 60 °C for 24 h. Ultrathin sections were prepared using an RMC MT-X ultramicrotome, placed on copper grids and examined using a transmission electron microscope (H-7100; Hitachi, Tokyo, Japan).

2.9. Luciferase activity

PDAC cells were co-transfected with a combination of either a negative control miRNA or a mimic of *miR-101* along with a luciferase reporter vector that included either a fragment of the wild-type 3′-UTR of the QKI (GUACUGUG)or a sequence containing mutations (CCCAAAAA). Following transfection 48 h, luciferase activity was measured using a dual-luciferase reporter assay kit (Beyotime, Shanghai).

2.10. Immunofluorescence staining

Cells were gathered and fixed with 4 % PFA, then rinsed with PBS before being permeabilized with Triton-X100 for 15 min. After PBS rinses, cells were incubated with antibodies against α-SAM (1:250, ab109197, abcam), FAP (1:200, ab314456, abcam), FSP1 (1:200, ab197896, abcam) or Beclin-1 (1:200, ab62557, abcam) at 4 °C for overnight, followed by incubation with Alexa Fluor 488. After three more PBS washes, 4′,6-diamidino-2-phenylindole (DAPI) was applied to stain the cell nuclei in the dark. The sections were then treated with a solution to quench fluorescence background and the images were captured using a fluorescence microscope.

2.11. Immunohistochemistry

Paraffin-embedded tissue sections, each 5 μm in thickness, underwent a standard dewaxing process followed by incubation in a graded series of ethanol solutions to remove any residual wax. The sections were then briefly treated with ethylenediaminetetraacetic acid (EDTA) solution at a pH of 9.0 for 3 min to facilitate antigen retrieval. Following this, endogenous peroxidase activity was quenched using 3 % methanol hydrogen peroxide. The sections were subsequently incubated with a primary antibody for QKI or Beclin-1 at a dilution of 1:200 and incubated at 4 °C to bind overnight. Then, unbound antibodies were washed and the slides were treated with HRP-conjugated secondary antibodies. The presence of bound antibodies was visualized using a DAB

chromogen, which produced a brown precipitate. The nuclei were then counterstained with hematoxylin, a purple dye, to provide contrast. Afterward, the slides were dehydrated in a series of ethanol washes and cleared with xylene before being mounted with a coverslip. The stained sections were examined and imaged using a light microscope and QKI and Beclin-1 protein expression were analyzed.

2.12. Xenograft tumor model

Male BALB/c nude mice (6-week-old, 18–22 g) were purchased from Xi'an Jiaotong University Animal Research Center (Xian, China) and randomly divided into different groups (n = 5 for each group). The sample size for each experimental group (n = 5) was determined using a power analysis to ensure statistically robust results. A total of 5×10^6 Paca-2 cells were combined at a 1:1 ratio with *miR-101* stably transfected CAFs and injected into the right flank of 4-week-old BALB/c nude mice. After 7 days, the mice were given daily intraperitoneal injections of honokiol for 5 weeks. Tumor size was monitored weekly and all mice were sacrificed after 5 weeks. The maximum length (L) and minimum length (W) of the tumors were measured using a vernier caliper and the tumor volume was calculated as $(L \times W)^2/2$.

2.13. Statistical analysis

Data are expressed as the mean ± SD and the differences between groups were evaluated using GraphPad Prism 7.0 (GraphPad Software, USA) and SPSS 18.0 software. Significance between groups was determined using multivariate analysis of variance with Bonferroni corrections. The mean of the two samples was compared using the Student's *t*-test. $P < 0.05$ was considered statistically significant.

3. Results

3.1. CAF-specific miR-101 negatively correlates with QKI in PDAC

To investigate whether CAFs in the PDAC tumor microenvironment promote PDAC progression, we isolated and cultured primary CAFs and NFs from PDAC patient samples. Cell identity was confirmed by detecting established CAF marker proteins α-SMA, FAP, and FSP1. The results of immunofluorescence and Western blot analysis showed that the expression levels of α-SMA, FAP and FSP1 in CAF cells were higher than those in NF cells, which confirmed the successful isolation of CAFs from primary cultured tissues (Fig. 1A and B, $p<0.001$ and $p < 0.01$). Our previous study demonstrated that QKI is highly expressed in PDAC and contributes to CAF activation (Chu et al., 2019). Western blotting analysis revealed significantly elevated QKI protein expression in CAFs compared to NFs (Fig. 1C, $p < 0.001$). Using TargetScan software, we predicted *miR-101* potentially binding to the 3′-UTR of *QKI*. Given QKI's established role in CAF-mediated tumorigenesis across malignancies, we generated a mutant construct with disrupted binding sites (Fig. 1D). *MiR-101* expression was significantly lower in CAFs compared with NFs (Fig. 1E, $p < 0.001$). A dual luciferase reporter assay was used to further assess whether *QKI* is a direct target of *miR-101*. After *miR-101* overexpression, the relative luciferase activity of the wild-type *QKI* 3′-UTR

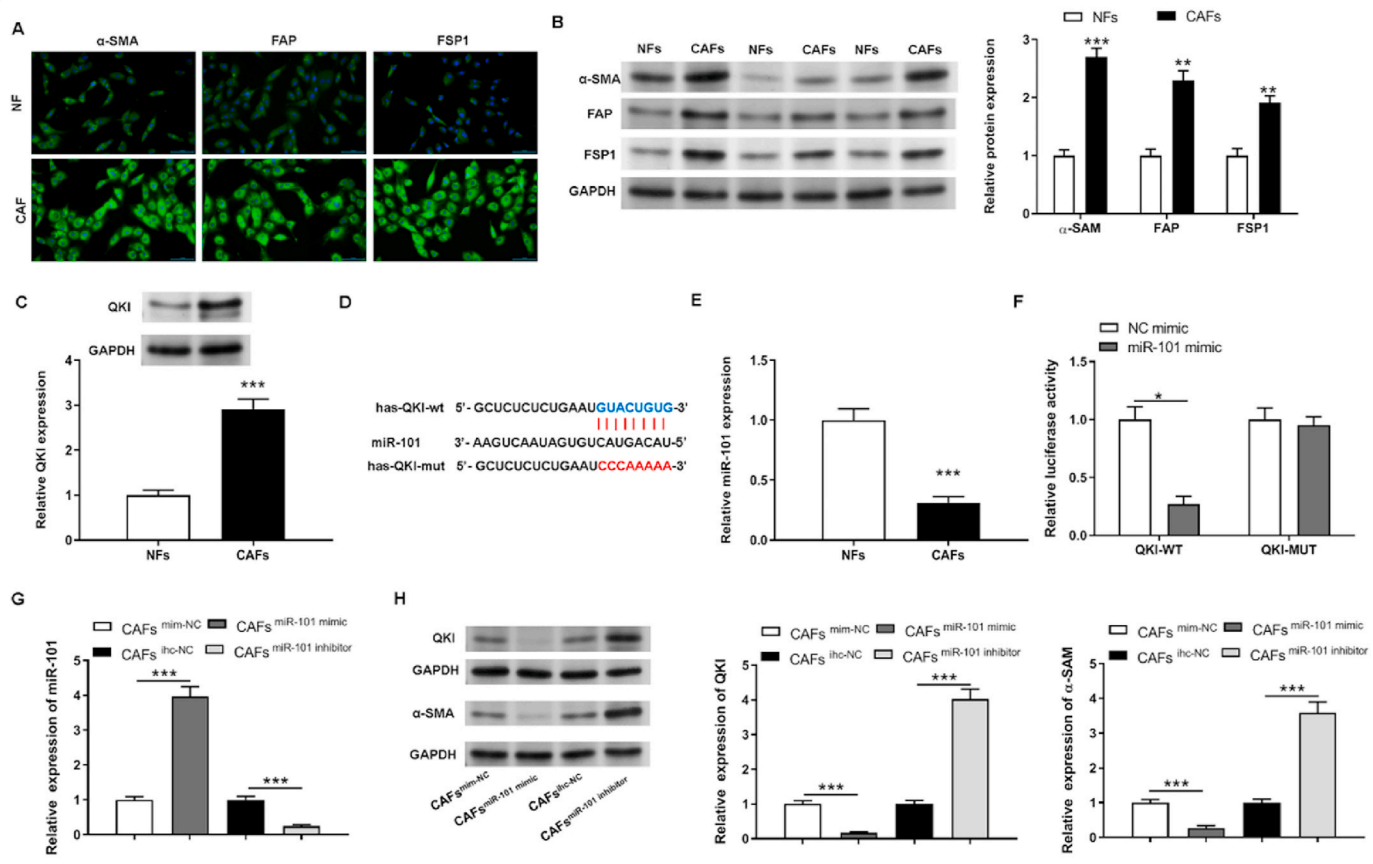

Fig. 1. QKI is a target of miR-101 in CAFs derived from PDAC tissues. (A, B) Immunofluorescence and western blotting analysis of α-SMA, FAP and FSP1 expression in paired NFs and CAFs. *Scale bar* = 100 μm. (C) Western blotting analysis of QKI expression in paired NFs and CAFs. (D) TargetScan prediction of the sequences of miR-101 containing the 3′-UTR QKI wild-type (wt) or mutant (mut) binding sites. (E) qRT-PCR analysis of *miR-101* expression in paired NFs and CAFs. (F) Luciferase activity of QKI-wt and *QKI*-mut in CAFs after transfecting cells with *miR-101* mimic or NC sequences. (G, H) Western blotting analysis of QKI and α-SMA expression in in CAFs after transfecting cells with *miR-101* mimic or inhibitor. The data are presented as the mean ± SD (n = 3). ***P < 0.001, **P < 0.01, *P < 0.05.

was significantly lower than that of the control, but the relative luciferase activity of the mutated *QKI* 3′-UTR was not (Fig. 1F, $p < 0.05$). Next, we assessed the regulatory effects of *miR-101* on QKI and α-SMA by transfecting *miR-101* mimic or inhibitor oligonucleotides into CAFs. The results show that transfecting CAFs with the *miR-101* mimic and inhibitor resulted in increased and decreased expression of *miR-101*, respectively (Fig. 1G, $p < 0.001$). MiR-101 overexpression reduced QKI and α-SMA levels, whereas miR-101 knockdown increased both proteins (Fig. 1H, $p < 0.001$).

3.2. Honokiol modulates the expression levels of miR-101, QKI and α-SMA in CAFs

Honokiol, a naturally compound with anti-cancer properties, inhibits tumor growth in PDAC. However, its potential impact on PDAC progression via interaction with CAFs is unknown. We investigated Honokiol's effects on *miR*-101 and its downstream targets in CAFs. Treatment with increasing concentrations of honokiol resulted in dose-dependent elevation of *miR-101* expression (Fig. 2A, $p < 0.001$, $p < 0.01$ and $p < 0.05$). Conversely, mRNA levels of QKI and α-SMA in CAFs decreased in a dose-dependent manner with increasing honokiol concentrations (Fig. 2B and C, $p < 0.001$, $p < 0.01$ and $p < 0.05$). Correspondingly, western blotting analysis confirmed a dose-dependent reduction in the protein levels of QKI and α-SMA (Fig. 2D, $p < 0.01$ and $p < 0.05$). These findings demonstrate that honokiol modulates the miR-101/QKI signaling axis in CAFs in a dose-dependent manner.

3.3. Honokiol inhibited CAFs-induced PDAC cell migration, invasion and autophagy

To investigate the effects of honokiol on CAF-responsive PDAC cell behavior, we treated CAFs with 25 or 50 μM honokiol, then collected the conditioned medium (CAF-CM) and assessed its ability to affect PDAC cells. We found that CAF-CM markedly suppressed cell viability of PANC-1 and Paca-2 cells (Fig. 3A, $p < 0.05$). Transwell migration assays revealed that CAF-CM from honokiol-treated cells suppressed the proliferation, migration and invasion ability of PDAC cells (Fig. 3B and C, $p < 0.05$). TEM and mRFP-GFP-LC3B reporter assays revealed that honokiol-treated CAF-CM inhibited autophagic flux in PDAC cells (Fig. 3D and E, $p < 0.05$). Furthermore, western blotting showed reduced LC3-II conversion, while immunofluorescence detected decreased Beclin-1 intensity in PDAC cells exposed to honokiol-treated CAF-CM (Fig. 3F and G, $p < 0.05$).

3.4. Honokiol contributes to miR-101 expression in CAFs to inhibit the malignant behavior of PDAC cells

To determine whether honokiol modulates PDAC cell behavior through CAF-derived miR-101, we performed functional assays using CAFs treated with honokiol (50 μM) and/or miR-101 inhibitor. The results revealed that PDAC cells exposed to honokiol-treated CAF-CM showed elevated miR-101 levels, which were abrogated by miR-101 inhibitor (Fig. 4A, $p < 0.01$). Co-treatment with miR-101 inhibitor reversed honokiol-mediated suppression of PANC-1 and Paca-2 cell proliferation, migration, and invasion (Fig. 4B–D, $p < 0.01$). Autophagic flux was monitored using mRFP-GFP-LC3 tandem fluorescence and Beclin-1 immunofluorescence. The results showed that *miR-101* inhibitor markedly improved the inhibitory impacts of honokiol-treated CAF-CM on autophagy (Fig. 4E and F, $p < 0.01$).

3.5. MiR-101 in CAFs modulates the malignant behavior of PDAC cells through reducing QKI

Since *miR-101* targets QKI 3′-UTR and suppress its expression, we examined its role in whether CAF-mediated PDAC pathogenesis through QKI regulation. QKI was markedly reduced in CAFs transfected with a *miR-101* mimic, but overexpression of *QKI* reversed this inhibitory effect (Fig. 5A, $p < 0.01$). Consistent with these results, overexpression of *QKI* in *miR-101*-overexpressing CAFs reduced the inhibitory effects on the proliferation, migration and invasion of PANC-1 and Paca-2 (Fig. 5B–D, $p < 0.05$). Additionally, miR-101-overexpressing CAFs reduced LC3 puncta formation and Beclin-1 intensity in PDAC cells, effects rescued by QKI overexpression (Fig. 5E and F).

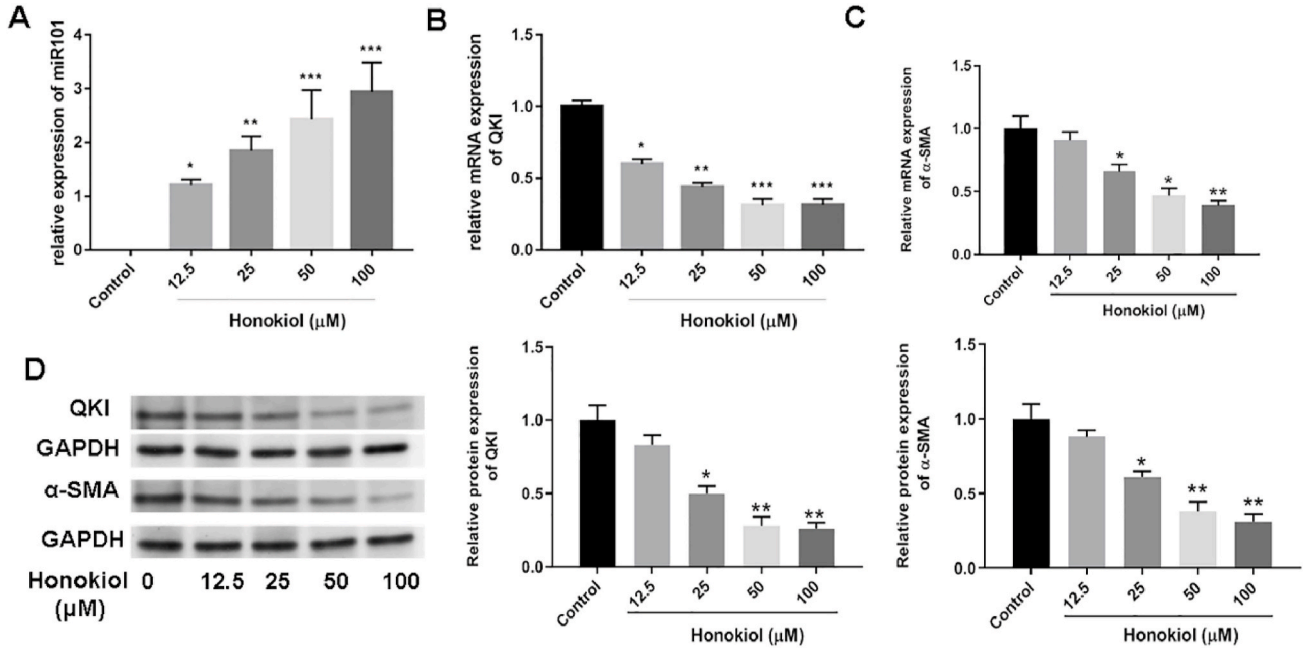

Fig. 2. Effect of Honokiol on the expression of *miR-101* and QKI in CAFs. CAFs were treated with increasing honokiol concentrations (0, 12.5, 25 and 50 μM). (A–C) qRT-PCR analysis of *miR-101* and the genes encoding QKI and α-SMA in CAFs treated with honokiol. (D) Western blot analysis of QKI and α-SMA expression in CAFs treated with honokiol. The data are presented as the mean ± SD (n = 3). ***P < 0.001, **P < 0.01, *P < 0.05.

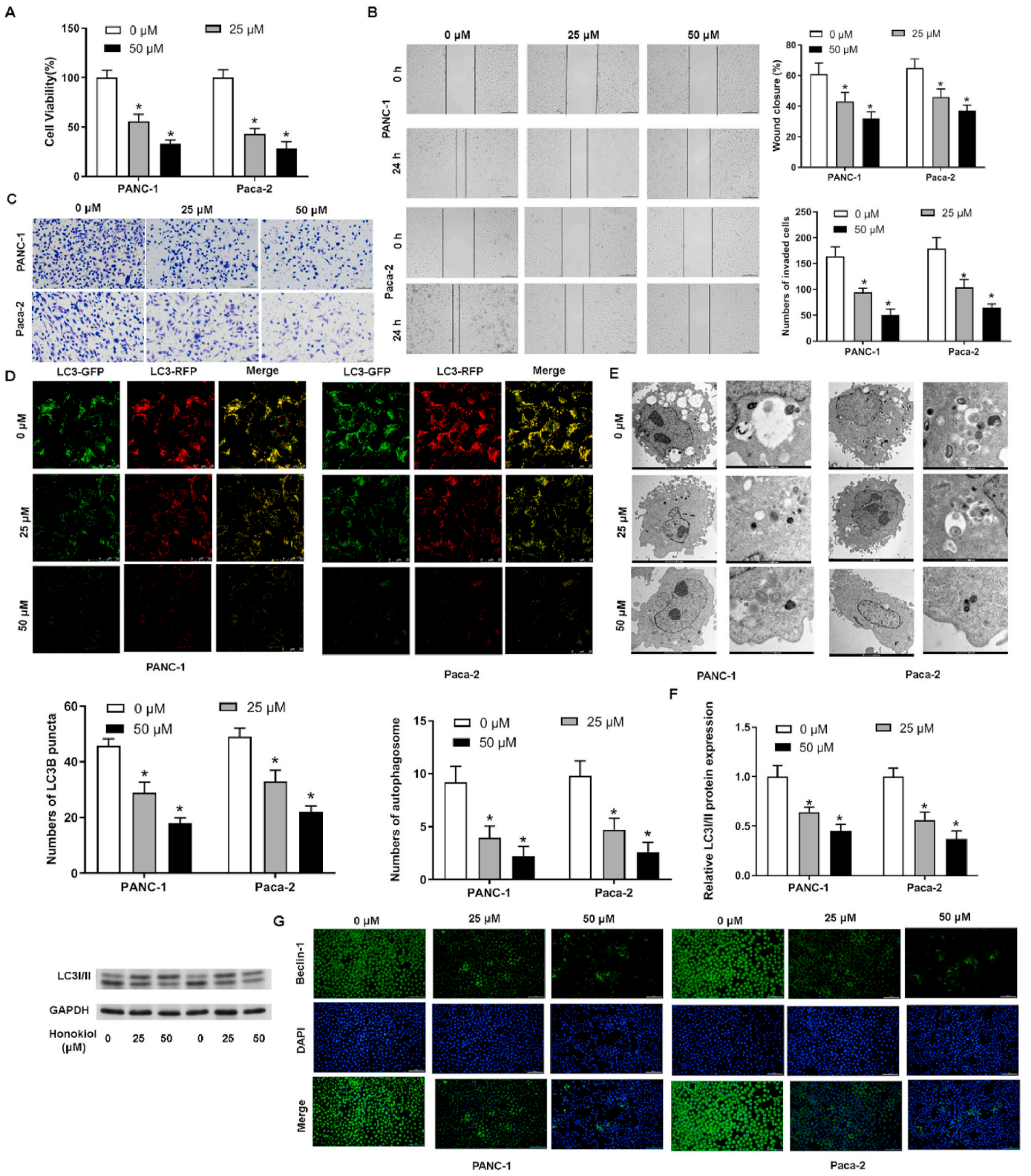

Fig. 3. The impact of honokiol on cell behavior in CAFs-treated PDAC cells. CAFs were treated with honokiol (25 or 50 μM) and then CAF-CM was collected and incubated with PDAC cells. (A) CCK-8 cell analysis viability of PDAC cells. (B, C) Wound healing and Transwell assays analysis cell migration and invasion of PDAC cells. *Scale bar* = 200 μm, *Scale bar* = 100 μm. (D) Immunofluorescence analysis following transfection of mRFP-GFP-LC3 into PDAC cells. *Scale bar* = 25 μm. (E) TEM analysis autolysosomes/autophagosomes of PDAC cells. *Scale bars* = 2 μm and 500 nm. (F, G) Western blotting and immunofluorescence analysis of LC3I/II and Beclin-1 in PDAC cells. *Scale bar* = 100 μm. The data are presented as the mean ± SD (n = 3). *P < 0.05.

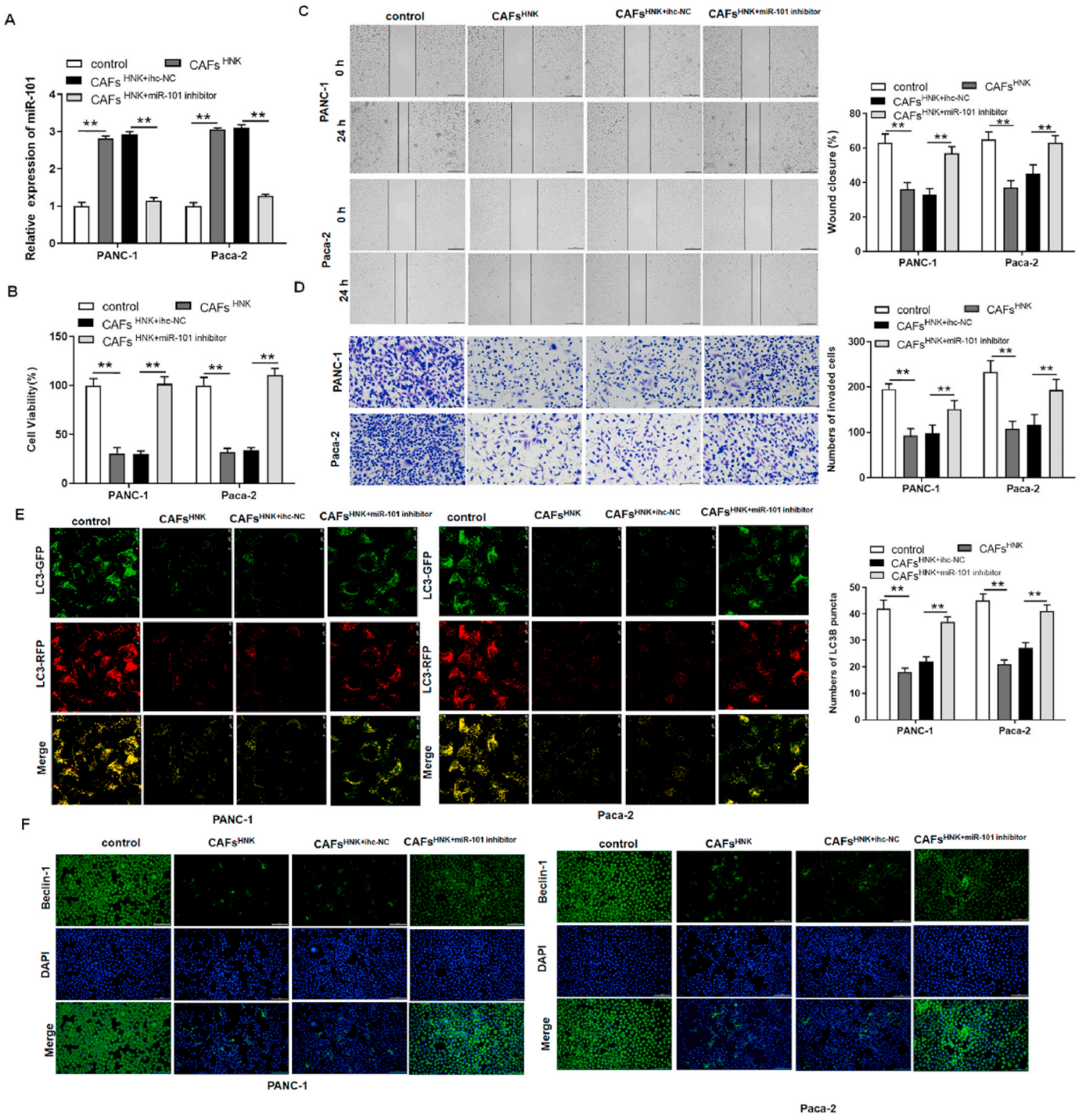

Fig. 4. The impact of honokiol on miR-101 secretion and expression in CAFs-treated PDAC cells. CAFs were treated with honokiol (50 μM) and transfected with *miR-101* inhibitor, then CAF-CM was incubated with PDAC cells. (A) qRT-PCR analysis of *miR-101* expression in PDAC cells. (B) CCK-8 cell analysis viability assay of PDAC cells. (C, D) Wound healing and Transwell assays analysis cell migration and invasion of PDAC cells. *Scale bars* = 200 μm; *Scale bars* = 100 μm. (E, F) Immunofluorescence analysis of mRFP-GFP-LC3 and Beclin-1 in PDAC cells. *Scale bars* = 25 μm and 100 μm. The data are presented as the mean ± SD (n = 3). **P < 0.01.

3.6. Honokiol inhibits CAFs-mediated tumor growth in nude mice by regulating miR-101/QKI axis

For *in vivo* validation, CAFs pre-transfected with miR-101 mimic or control were mixed with Paca-2 cells (1:1) and subcutaneously injected into nude mice. After 7 days, the mice were treated with daily injections of honokiol for 5 weeks. Honokiol-treated xenografts exhibited reduced tumor size and weight. The *miR-101* mimic combined with honokiol markedly increased the inhibitory effect of honokiol (Fig. 6A–C, $p<0.01$ and $p < 0.05$). Honokiol significantly enhanced *miR-101* expression in tumor tissues, and this promoting effect was further enhanced by transfection of *miR-101* mimic into CAFs (Fig. 6D, $p < 0.001$ and $p < 0.01$). In addition, IHC analysis revealed honokiol-mediated down-regulation of QKI and Beclin-1 protein in PDAC tumor tissues. This effect was enhanced in mice receiving miR-101 mimic-transfected CAFs (Fig. 6E).

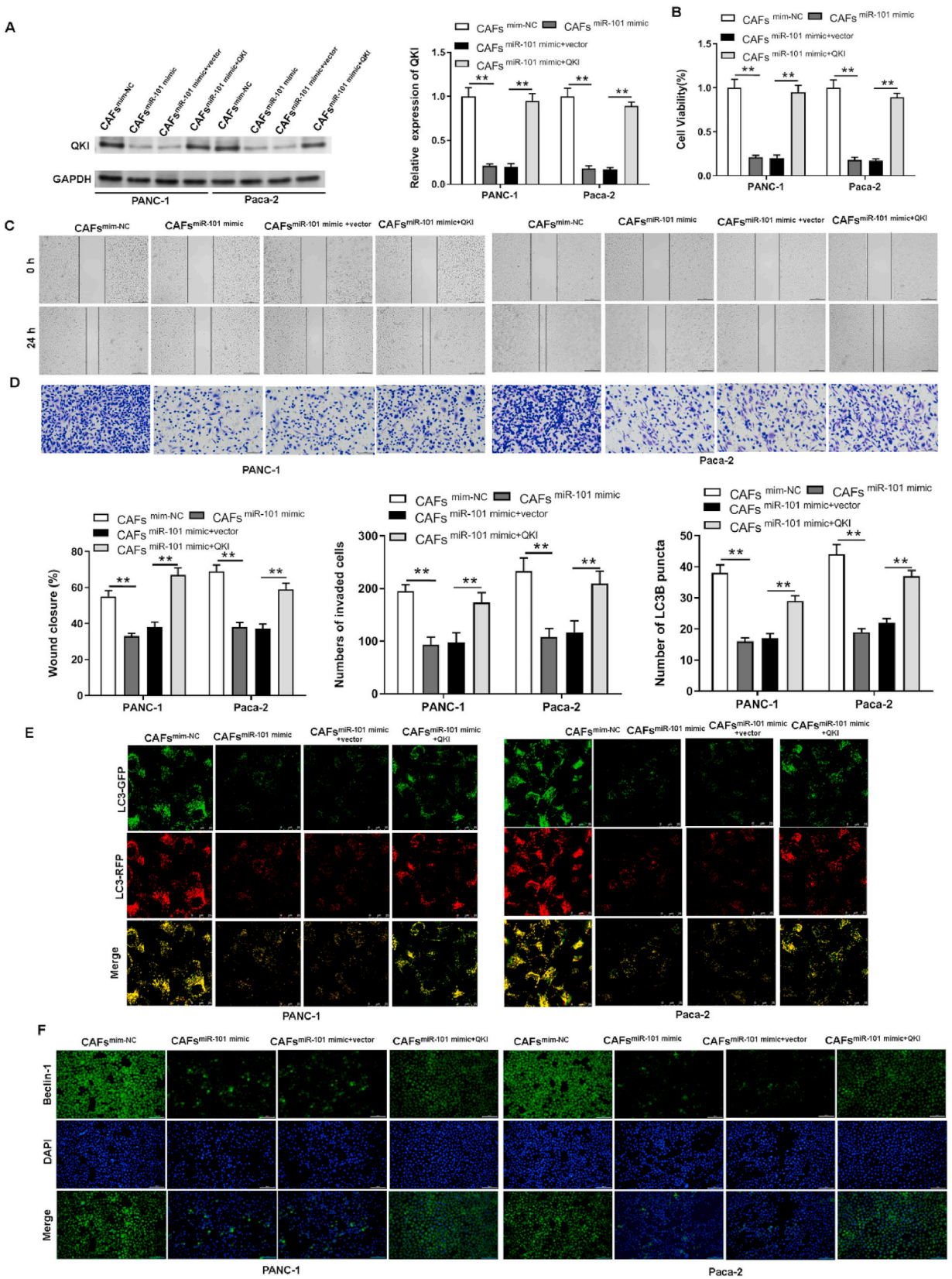

Fig. 5. QKI is a target of *miR-101* in CAFs. CAFs were transfected with *miR-101* mimic or/and *QKI*, then CAF-CM was collected and incubated with PDAC cells. (A) Western blotting analysis of QKI expression in PDAC cells. (B) CCK-8 cell analysis viability of PDAC cells. (C, D) Wound healing and Transwell assays analysis cell migration and invasion of PDAC cells. *Scale bars* = 200 μm; *Scale bars* = 100 μm. (E, F) Immunofluorescence analysis of mRFP-GFP-LC3 and Beclin-1 in PDAC cells. *Scale bars* = 25 μm; *Scale bars* = 100 μm **P < 0.01.

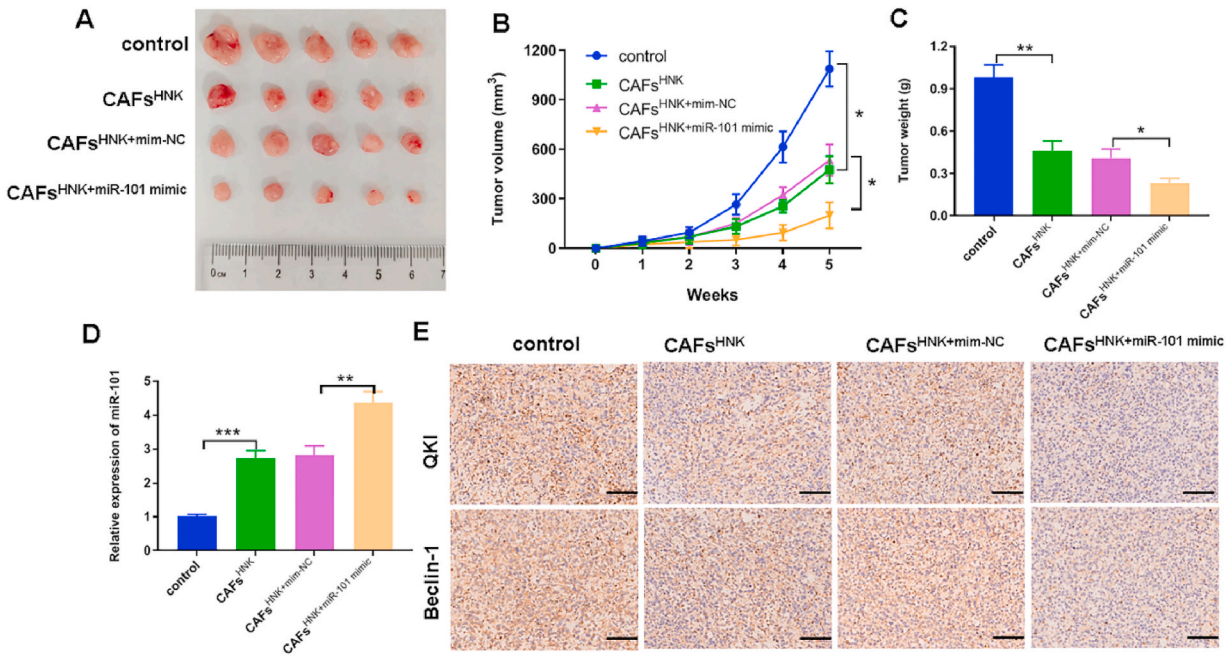

Fig. 6. Honokiol regulates the *miR-101*/QKI signaling axis to inhibit tumor growth. CAFs were treated with honokiol and transfected with either *miR-101* mimic or inhibitor, then mixed with Paca-2 cells at a ratio of 1:1 and injected into the flank of nude mice. The tumors were allowed to establish for 7 days, then the mice were treated daily with intraperitoneally injections of the honokiol for 35 days. The mice were then sacrificed and tumors were collected and analyzed. (A) Representative images of the xenograft tumors (n = 5). (B, C) The tumor volume and weight were measured in mice every 7 days (n = 5). (D) qRT-PCR analysis of *miR-101* expression in xenograft tumor tissues (n = 5). (E) Immunohistochemistry analysis of QKI and Beclin-1 protein levels in xenograft tumor tissues (n = 5). *Scale bars* = 50 μm. The data are presented as the mean ± SD (n = 5). ***P < 0.001, **P < 0.01, *P < 0.05.

4. Discussion

The high invasion and drug resistance of PDAC hinder the effective treatment of PDAC. The surrounding stroma of PDAC has become a promising research direction for studying the disease process of PDAC due to its large proportion (up to 80–90 % of the surrounding tissue). The strategy of targeting the tumor stroma to improve therapeutic outcomes in PDAC has gained considerable traction. Several approaches have been explored, including the direct depletion of CAFs (e.g., using a hedgehog pathway inhibitor IPI-926 or FAP-targeting therapies), inhibition of stromal-derived signaling (e.g., targeting CXCR4, CCR2, or TGF-β pathways), and disruption of the dense extracellular matrix (e.g., with PEGPH20 to degrade hyaluronan) (Seki et al., 2022; Özdemir et al., 2015). As an important part of the TME, the interaction between CAFs and tumor may become a key factor modulating PDAC tumorigenesis, but its potential mechanism is not clear.

Honokiol has been reported to have anti-tumor activity, and its mechanism of action involves multiple molecular targets and signaling pathways. Honokiol can affect the TME through a variety of mechanisms, such as anti-angiogenesis, anti-tumor immune response and anti-inflammatory effects, which impact the metabolism of tumor cells (Cho et al., 2015; Fried & Arbiser, 2009; Jiraviriyakul et al., 2019; Yi et al., 2022). In addition, honokiol is involved in PDAC development and metastasis through multiple mechanisms. For example, honokiol can inhibit invasion, migration and perineural invasion of pancreatic cancer by blocking SMAD2/3 phosphorylation (Qin et al., 2021). Honokiol contributes to the apoptosis of PDAC cells by inhibiting the expression of cyclin and promoting apoptotic proteins (Arora et al., 2011). Surprisingly, researchers have found that honokiol can inhibit the expression of α-SMA and collagen I in tumor tissues, thereby preventing the pro-fibrotic response and reducing the growth and metastasis of PDAC tumors (Averett et al., 2016). However, little is known about the role of honokiol in CAFs-mediated tumor development in the TME. In this study, we isolated CAFs from PDAC patients. Treatment with honokiol altered the function of CAFs to inhibit their ability to promote PDAC tumor proliferation, migration, invasion and autophagy. Mechanistically, we found that honokiol could enhance *miR-101* expression, which is consistent with previous findings (Wang, Liu, et al., 2020).

Cancer cell-derived miRNAs regulate the TME via non-cell autonomous mechanisms, inducing adjacent cells to acquire oncogenic miRNAs expression profiles. This highlights the critical role of TME miRNAs in modulating the behavior of cancer cells. As key regulators of signaling pathways, miRNAs represent promising therapeutic targets for remodeling CAFs. In the context of CAFs, the role of *miR-101* has attracted particular attention from researchers. In lung cancer CAFs, *miR-101* is the most downregulated miRNA and impairs CAF-tumor cell crosstalk by inhibiting the expression of CXCL12 (Zhang, Liu, et al., 2015). *MiR-101* could inhibit the formation of vascular mimicry by regulating the expression of extracellular matrix-related genes in CAFs, such as VE-cadherin and MMP2, through the TGF-β/SDF1 axis (Yang et al., 2016). Downregulated in hepatocellular carcinoma (HCC) CAFs, *miR-101* correlates with poor prognosis of HCC patients and targets TGFBR1 to regulate the phosphorylation of SMAD2/3 (Eun et al., 2023). Here, we found that*miR-101* was expressed at low levels in PDAC-CAFs compared with NFs. Honokiol treatment upregulated miR-101 in CAFs, and CAF-CM from honokiol-treated cells impaired PDAC cell proliferation, migration, invasion, and autophagic flux. These inhibitory effects were abrogated by *miR-101* inhibitor. Our earlier study established that QKI contributes to CAF activation and PDAC tumorigenesis (Chu et al., 2019). In this study, we found that the 3′-UTR of *QKI* was a target of *miR-101* in CAFs, suggesting that *miR-101* directly regulates *QKI* expression levels.

QKI (Quaking), an RNA-binding protein in the GLD-2 glycosidase family, regulates RNA processing, splicing and transport. QKI has been found to function in a variety of biological processes and has been identified as an important molecule in cancer research, especially in the context of PDAC. Elevated QKI expression in primary and metastatic PDAC tumors correlates with basal-like phenotype, contributing to PDAC cell migration, chemoresistance, and reducing patient survival (Ruta et al., 2024). In PDAC containing KRAS-mutations, QKI was

reported to increase the expression of *circARFGEF2* through alternative splicing, which led to JAK2-STAT3 pathway activation and triggered lymph node metastasis (Kong et al., 2023). We identified miR-101 as a negative regulator of QKI that suppresses CAF activation. Overexpression of QKI in CAFs reversed the effect of *miR-101* on the malignant behaviors of PDAC cells, further confirming that QKI was a target gene of *miR-101* and was involved in the process of *miR-101*-regulated PDAC cell proliferation, invasion and autophagy. While our *in vitro* findings provide robust mechanistic insights, they are primarily based on two widely used PDAC cell lines, PANC-1 and Paca-2. Although these lines are well-established models representing key features of PDAC, they cannot fully capture the immense genetic and phenotypic heterogeneity inherent to human pancreatic cancer. Besides, our xenograft model provides valuable mechanistic insights into the honokiol/miR-101/QKI axis, we acknowledge the inherent limitations in translating these findings directly to the clinical setting of human PDAC. Future studies employing more advanced models, such as patient-derived organoids (PDOs), patient-derived xenografts (PDXs) that retain the human stromal compartment, or immunocompetent genetically engineered mouse models (GEMMs) of PDAC.

In summary, honokiol modulated the CAF miR-101/QKI axis, exerting antitumor effects in PDAC. Our data suggested that honokiol alleviated tumor growth by inhibiting PDAC cell proliferation, migration, invasion and autophagy. As a natural compound with a known safety profile and the ability to target multiple oncogenic pathways simultaneously, honokiol offers a multi-faceted approach that could be more effective than single-target agents and may synergize with existing chemotherapy regimens like gemcitabine or nab-paclitaxel. Although additional studies are warranted, honokiol shows promise as a PDAC adjuvant therapy that remodels the TME to potentiate conventional treatments.

CRediT authorship contribution statement

Liang Chu: Investigation, Data curation, Conceptualization. **Bin Yu:** Writing – review & editing, Methodology, Formal analysis. **Zhe Jiang:** Methodology, Investigation, Formal analysis. **Zan Liu:** Writing – review & editing, Validation, Supervision. **Yunmei Wang:** Writing – review & editing, Writing – original draft, Data curation, Conceptualization. **Yuqin Hu:** Writing – review & editing, Writing – original draft, Methodology, Data curation.

Data availability statement

The datasets used during the present study are available from the corresponding author upon reasonable request.

Funding

The present study was supported by the Basic Research on Natural Sciences in Shaanxi Province(No. S2023-JC-YB-2701).

Conflicts of interest

No conflicts of interest exist in the submission of this manuscript.

Acknowledgments

None.

References

Arora, S., Bhardwaj, A., Srivastava, S. K., Singh, S., McClellan, S., Wang, B., & Singh, A. P. (2011). Honokiol arrests cell cycle, induces apoptosis, and potentiates the cytotoxic effect of gemcitabine in human pancreatic cancer cells. *PLoS One, 6*(6), Article e21573. https://doi.org/10.1371/journal.pone.0021573

Arora, S., Singh, S., Piazza, G. A., Contreras, C. M., Panyam, J., & Singh, A. P. (2012). Honokiol: A novel natural agent for cancer prevention and therapy. *Current Molecular Medicine, 12*(10), 1244–1252. https://doi.org/10.2174/156652412803833508

Averett, C., Bhardwaj, A., Arora, S., Srivastava, S. K., Khan, M. A., Ahmad, A., … Singh, A. P. (2016). Honokiol suppresses pancreatic tumor growth, metastasis and desmoplasia by interfering with tumor-stromal cross-talk. *Carcinogenesis, 37*(11), 1052–1061. https://doi.org/10.1093/carcin/bgw096

Avtanski, D. B., Nagalingam, A., Bonner, M. Y., Arbiser, J. L., Saxena, N. K., & Sharma, D. (2014). Honokiol inhibits epithelial-mesenchymal transition in breast cancer cells by targeting signal transducer and activator of transcription 3/Zeb1/E-cadherin axis. *Molecular Oncology, 8*(3), 565–580. https://doi.org/10.1016/j.molonc.2014.01.004

Beutel, A. K., & Halbrook, C. J. (2023). Barriers and opportunities for gemcitabine in pancreatic cancer therapy. *American journal of physiology Cell physiology, 324*(2), C540–c552. https://doi.org/10.1152/ajpcell.00331.2022

Biffi, G., & Tuveson, D. A. (2021). Diversity and biology of cancer-associated fibroblasts. *Physiological Reviews, 101*(1), 147–176. https://doi.org/10.1152/physrev.00048.2019

Carthew, R. W., & Sontheimer, E. J. (2009). Origins and mechanisms of miRNAs and siRNAs. *Cell, 136*(4), 642–655. https://doi.org/10.1016/j.cell.2009.01.035

Chapman, N. M., & Chi, H. (2024). Metabolic rewiring and communication in cancer immunity. *Cell Chemical Biology, 31*(5), 862–883. https://doi.org/10.1016/j.chembiol.2024.02.001

Cho, J. H., Jeon, Y. J., Park, S. M., Shin, J. C., Lee, T. H., Jung, S., … Chae, J. I. (2015). Multifunctional effects of honokiol as an anti-inflammatory and anti-cancer drug in human oral squamous cancer cells and xenograft. *Biomaterials, 53*, 274–284. https://doi.org/10.1016/j.biomaterials.2015.02.091

Chu, L., Hu, Y., Jiang, Y. H., Xu, C., Liu, W. C., & Lu, Z. F. (2019). Effects of RNA binding protein QKI on pancreatic cancer ductal epithelial cells and surrounding activation fibroblasts. *Journal of Cellular Biochemistry, 120*(7), 11551–11561. https://doi.org/10.1002/jcb.28435

DeSantis, C. E., Lin, C. C., Mariotto, A. B., Siegel, R. L., Stein, K. D., Kramer, J. L., … Jemal, A. (2014). Cancer treatment and survivorship statistics, 2014. *CA: a cancer journal for clinicians, 64*(4), 252–271. https://doi.org/10.3322/caac.21235

Dragomir, M. P., Knutsen, E., & Calin, G. A. (2022). Classical and noncanonical functions of miRNAs in cancers. *Trends in Genetics: Trends in Genetics, 38*(4), 379–394. https://doi.org/10.1016/j.tig.2021.10.002

Eun, J. W., Ahn, H. R., Baek, G. O., Yoon, M. G., Son, J. A., Weon, J. H., … Cho, H. J. (2023). Aberrantly expressed MicroRNAs in cancer-associated fibroblasts and their target oncogenic signatures in hepatocellular carcinoma. *International Journal of Molecular Sciences, 24*(5). https://doi.org/10.3390/ijms24054272

Fang, Y., Tan, C., Zheng, Z., Yang, J., Tang, J., Guo, R., … Wang, Y. (2025). The function of microRNA related to cancer-associated fibroblasts in pancreatic ductal adenocarcinoma. *Biochemical Pharmacology, 236*, Article 116849. https://doi.org/10.1016/j.bcp.2025.116849

Fried, L. E., & Arbiser, J. L. (2009). Honokiol, a multifunctional antiangiogenic and antitumor agent. *Antioxidants and Redox Signaling, 11*(5), 1139–1148. https://doi.org/10.1089/ars.2009.2440

Gillen, S., Schuster, T., Meyer Zum Büschenfelde, C., Friess, H., & Kleeff, J. (2010). Preoperative/Neoadjuvant therapy in pancreatic cancer: A systematic review and meta-analysis of response and resection percentages. *PLoS Medicine, 7*(4), Article e1000267. https://doi.org/10.1371/journal.pmed.1000267

Hosein, A. N., Brekken, R. A., & Maitra, A. (2020). Pancreatic cancer stroma: An update on therapeutic targeting strategies. *Nature Reviews Gastroenterology & Hepatology, 17*(8), 487–505. https://doi.org/10.1038/s41575-020-0300-1

Huang, J. S., Yao, C. J., Chuang, S. E., Yeh, C. T., Lee, L. M., Chen, R. M., … Lai, G. M. (2016). Honokiol inhibits sphere formation and xenograft growth of oral cancer side population cells accompanied with JAK/STAT signaling pathway suppression and apoptosis induction. *BMC Cancer, 16*, 245. https://doi.org/10.1186/s12885-016-2265-6

Jiraviriyakul, A., Songjang, W., Kaewthet, P., Tanawatkitichai, P., Bayan, P., & Pongcharoen, S. (2019). Honokiol-enhanced cytotoxic T lymphocyte activity against cholangiocarcinoma cells mediated by dendritic cells pulsed with damage-associated molecular patterns. *World Journal of Gastroenterology, 25*(29), 3941–3955. https://doi.org/10.3748/wjg.v25.i29.3941

Kim, S. Y., Jo, M. J., Yoon, M. S., Jin, C. E., Shin, Y. B., Lee, J. M., … Shin, D. H. (2023). Gemcitabine and rapamycin-loaded mixed polymeric thermogel for metastatic pancreatic cancer therapy. *Journal of Controlled Release: Official Journal of the Controlled Release Society, 360*, 796–809. https://doi.org/10.1016/j.jconrel.2023.07.010

Kong, Y., Luo, Y., Zheng, S., Yang, J., Zhang, D., Zhao, Y., … Chen, R. (2023). Mutant KRAS mediates circARFGEF2 biogenesis to promote lymphatic metastasis of pancreatic ductal adenocarcinoma. *Cancer Research, 83*(18), 3077–3094. https://doi.org/10.1158/0008-5472.can-22-3997

Li, Q., Zhang, D., Wang, Y., Sun, P., Hou, X., Larner, J., … Mi, J. (2013). MiR-21/Smad 7 signaling determines TGF-β1-induced CAF formation. *Scientific Reports, 3*, 2038. https://doi.org/10.1038/srep02038

Melstrom, L. G., Salazar, M. D., & Diamond, D. J. (2017). The pancreatic cancer microenvironment: A true double agent. *Journal of Surgical Oncology, 116*(1), 7–15. https://doi.org/10.1002/jso.24643

Miller, K. D., Goding Sauer, A., Ortiz, A. P., Fedewa, S. A., Pinheiro, P. S., Tortolero-Luna, G., … Siegel, R. L. (2018). Cancer statistics for hispanics/latinos, 2018. *CA: a cancer journal for clinicians, 68*(6), 425–445. https://doi.org/10.3322/caac.21494

New, J., & Thomas, S. M. (2019). Autophagy-dependent secretion: Mechanism, factors secreted, and disease implications. *Autophagy, 15*(10), 1682–1693. https://doi.org/10.1080/15548627.2019.1596479

Niu, N., Shen, X., Wang, Z., Chen, Y., Weng, Y., Yu, F., … Xue, J. (2024). Tumor cell-intrinsic epigenetic dysregulation shapes cancer-associated fibroblasts heterogeneity to metabolically support pancreatic cancer. *Cancer Cell, 42*(5), 869–884.e869. https://doi.org/10.1016/j.ccell.2024.03.005

Özdemir, B. C., Pentcheva-Hoang, T., Carstens, J. L., Zheng, X., Wu, C. C., Simpson, T. R., … Kalluri, R. (2015). Depletion of carcinoma-associated fibroblasts and fibrosis induces immunosuppression and accelerates pancreas cancer with reduced survival. *Cancer Cell, 28*(6), 831–833. https://doi.org/10.1016/j.ccell.2015.11.002

Peng, Y., Zhang, X., Feng, X., Fan, X., & Jin, Z. (2017). The crosstalk between microRNAs and the Wnt/β-catenin signaling pathway in cancer. *Oncotarget, 8*(8), 14089–14106. https://doi.org/10.18632/oncotarget.12923

Qin, T., Li, J., Xiao, Y., Wang, X., Gong, M., Wang, Q., … Sha, H. (2021). Honokiol suppresses perineural invasion of pancreatic cancer by inhibiting SMAD2/3 signaling. *Frontiers in oncology, 11*, Article 728583. https://doi.org/10.3389/fonc.2021.728583

Rebelo, R., Xavier, C. P. R., Giovannetti, E., & Vasconcelos, M. H. (2023). Fibroblasts in pancreatic cancer: Molecular and clinical perspectives. *Trends in Molecular Medicine, 29*(6), 439–453. https://doi.org/10.1016/j.molmed.2023.03.002

Ruta, V., Naro, C., Pieraccioli, M., Leccese, A., Archibugi, L., Cesari, E., … Sette, C. (2024). An alternative splicing signature defines the basal-like phenotype and predicts worse clinical outcome in pancreatic cancer. *Cell Reports Medicine, 5*(2), Article 101411. https://doi.org/10.1016/j.xcrm.2024.101411

Seki, T., Saida, Y., Kishimoto, S., Lee, J., Otowa, Y., Yamamoto, K., … Brender, J. R. (2022). PEGPH20, a PEGylated human hyaluronidase, induces radiosensitization by reoxygenation in pancreatic cancer xenografts. A molecular imaging study. *Neoplasia, 30*, Article 100793. https://doi.org/10.1016/j.neo.2022.100793

Shen, Z., Qin, X., Yan, M., Li, R., Chen, G., Zhang, J., & Chen, W. (2017). Cancer-associated fibroblasts promote cancer cell growth through a miR-7-RASSF2-PAR-4 axis in the tumor microenvironment. *Oncotarget, 8*(1), 1290–1303. https://doi.org/10.18632/oncotarget.13609

Shen, H., Yu, X., Yang, F., Zhang, Z., Shen, J., Sun, J., … Shu, Y. (2016). Reprogramming of normal fibroblasts into cancer-associated fibroblasts by miRNAs-Mediated CCL2/VEGFA signaling. *PLoS Genetics, 12*(8), Article e1006244. https://doi.org/10.1371/journal.pgen.1006244

Shi, Y., Gao, W., Lytle, N. K., Huang, P., Yuan, X., Dann, A. M., … Hunter, T. (2019). Targeting LIF-Mediated paracrine interaction for pancreatic cancer therapy and monitoring. *Nature, 569*(7754), 131–135. https://doi.org/10.1038/s41586-019-1130-6

Thomas, D., & Radhakrishnan, P. (2019). Tumor-stromal crosstalk in pancreatic cancer and tissue fibrosis. *Molecular Cancer, 18*(1), 14. https://doi.org/10.1186/s12943-018-0927-5

Wang, Y., Liu, Z., Liu, Q., Han, Y., Zang, Y., Zhang, H., … Wu, Y. (2020). Honokiol suppressed pancreatic cancer progression via miR-101/Mcl-1 axis. *Cancer Management and Research, 12*, 5243–5254. https://doi.org/10.2147/cmar.s237323

Wang, Q., Yang, Y., Lu, G., Sun, X., Feng, Y., Yan, S., … Chen, R. (2020). Genome-wide identification of microRNAs and phased siRNAs in soybean roots under long-term salt stress. *Genes & genomics, 42*(11), 1239–1249. https://doi.org/10.1007/s13258-020-00990-0

Yang, J., Lu, Y., Lin, Y. Y., Zheng, Z. Y., Fang, J. H., He, S., & Zhuang, S. M. (2016). Vascular mimicry formation is promoted by paracrine TGF-β and SDF1 of cancer-associated fibroblasts and inhibited by miR-101 in hepatocellular carcinoma. *Cancer letters, 383*(1), 18–27. https://doi.org/10.1016/j.canlet.2016.09.012

Yi, X., Qi, M., Huang, M., Zhou, S., & Xiong, J. (2022). Honokiol inhibits HIF-1α-Mediated glycolysis to halt breast cancer growth. *Frontiers in Pharmacology, 13*, Article 796763. https://doi.org/10.3389/fphar.2022.796763

Zhang, J., Liu, J., Liu, Y., Wu, W., Li, X., Wu, Y., … Gu, L. (2015). miR-101 represses lung cancer by inhibiting interaction of fibroblasts and cancer cells by down-regulating CXCL12. *Biomedicine & pharmacotherapy = Biomedecine & pharmacotherapie, 74*, 215–221. https://doi.org/10.1016/j.biopha.2015.08.013

Zhang, Q., Zhao, W., Ye, C., Zhuang, J., Chang, C., Li, Y., … Yan, J. (2015). Honokiol inhibits bladder tumor growth by suppressing EZH2/miR-143 axis. *Oncotarget, 6*(35), 37335–37348. https://doi.org/10.18632/oncotarget.6135